Effects of electron-boundary scattering on changes in thermoreflectance in thin metal films undergoing intraband excitations

Patrick E. Hopkins

Related Articles

Thermal conductivity of nano-grained SrTiO3 thin films
Appl. Phys. Lett. 101, 231908 (2012)

Thermal conductivity of silicon nanowire arrays with controlled roughness
J. Appl. Phys. 112, 114306 (2012)

Parametric study of the frequency-domain thermoreflectance technique
J. Appl. Phys. 112, 103105 (2012)

Thermo-optical properties of embedded silver nanoparticles
J. Appl. Phys. 112, 103101 (2012)

Role of phonon anharmonicity in time-domain thermoreflectance measurements
Appl. Phys. Lett. 101, 083108 (2012)

Additional information on J. Appl. Phys.

Journal Homepage: http://jap.aip.org/

Journal Information: http://jap.aip.org/about/about_the_journal

Top downloads: http://jap.aip.org/features/most_downloaded

Information for Authors: http://jap.aip.org/authors

Effects of electron-boundary scattering on changes in thermoreflectance in thin metal films undergoing intraband excitations

Patrick E. Hopkins[a)]

Engineering Sciences Center, Sandia National Laboratories, P.O. Box 5800, Albuquerque, New Mexico 87185-0346, USA

As characteristic sizes and lengths scales continue to decrease in nanostructures, carrier scattering processes at the geometric boundaries and interfaces in nanosystems become more prevalent. These scattering events can lead to additional resistances. This paper investigates electron-boundary scattering processes by examining changes in thermoreflectance signals in thin films after short pulsed laser heating. To take electron-boundary scattering into account, an additional scattering term is introduced into the Drude model for the complex dielectric function. Using an intraband thickness-dependent reflectance model, transient thermoreflectance data of Au films subject to intraband excitations are analyzed with the electron-boundary scattering Drude model introduced in this work. The electron-boundary scattering rate is determined from Au thermoreflectance data, showing that after short pulsed laser heating, electron-boundary scattering rates can be almost three orders of magnitude greater than the electron-electron and electron-phonon scattering rates. The scattering rates determined from the thermoreflectance data agree well with the theoretical predictions for electron-boundary scattering calculated from an electron-boundary scattering model for disordered conductors in the event of an electron-phonon nonequilibrium. © *2009 American Institute of Physics*. [DOI: 10.1063/1.3117486]

I. INTRODUCTION

Heat transfer in nanostructures is drastically altered by carrier scattering events.[1] As characteristic sizes and lengths scales continue to decrease, the carrier scattering processes at the geometric boundaries and interfaces in nanosystems become more prevalent. These scattering events can lead to additional resistances, leading to hot spots and device heating, and must be understood to effectively engineer nanomaterial systems.

In metal and doped semiconductor systems, thermal transport and resistances are governed by electron scattering events such as electron-electron and electron-phonon interactions. These electronic processes can be observed via photonic excitations and reflectance monitoring. A common technique to measure electron-electron and electron-phonon interactions and thermalization times is the pump-probe transient thermoreflectance (TTR) technique.[2–10] In the TTR technique, the change in reflectance of the surface of a metal film, ΔR, is measured after a short pulse heating event. This change in reflectance is related to the various electron-electron and electron-phonon scattering processes, and ΔR can be used to determine the rates of these scattering processes. In films with thicknesses on the order of the electron mean free path, electron-boundary scattering at the film/substrate interface can affect ΔR,[7] and in this case, ΔR is related to electron-boundary scattering rates.

In this work, ΔR in metal films is studied after intraband electron excitations. The reflectance models for ΔR developed in this work use multiple reflection theory to account for photon-substrate interactions and how this interaction af-fects pulse energy absorption in the metal film. The dependency of ΔR on electron-electron, electron-phonon, and electron-substrate scattering rates as a function of electron temperature is studied by modifying the Drude model for the intraband component of the dielectric function. The modified Drude model is used to develop an intraband reflectance model for ΔR that accounts for electron-boundary scattering. Electron-boundary scattering rates are deduced by comparing the thermoreflectance model to TTR data on thin Au films on Si and glass (SiO_2) substrates. The electron-boundary scattering rates determined from ΔR are compared to a model for electron-boundary scattering during an electron-phonon nonequilibrium that is derived in this work.

II. $\Delta R/R$ AFTER INTRABAND EXCITATIONS IN THIN FILMS

In thermoreflectance experiments, it is the change in reflectivity ΔR resulting from a change in temperature in the sample which is measured. The change in reflectance of a metal can be related to the change in temperature through the change in the complex dielectric function $\Delta\varepsilon(\omega,\Delta T) = \Delta\varepsilon_1(\omega,\Delta T) + i\Delta\varepsilon_2(\omega,\Delta T)$, where $\Delta\varepsilon_1(\omega,\Delta T)$ and $\Delta\varepsilon_2(\omega,\Delta T)$ are the changes in the real and imaginary parts of the complex dielectric function, respectively.[11] For ultrashort laser pulses with pulse widths less than the electron-phonon thermalization time ($t_{\text{pulse}} < \tau_{\text{ep}}$), the resulting reflectance, and thus the dielectric function, is a function of both the change in electron and phonon temperatures ΔT_e and ΔT_p: $\Delta\varepsilon(\omega,\Delta T_e,\Delta T_p) = \Delta\varepsilon_1(\omega,\Delta T_e,\Delta T_p) + i\Delta\varepsilon_2(\omega,\Delta T_e,\Delta T_p)$. For small changes in temperature, ($\Delta T_e, \Delta T_p < 150$ K), $\Delta\varepsilon$ can be expressed as a linear change in ΔT_e and ΔT_p,[3,12,13]

[a)]Electronic mail: pehopki@sandia.gov.

$$\Delta\varepsilon = \Delta\varepsilon_1 + i\Delta\varepsilon_2 = \frac{\partial\varepsilon_1}{\partial T_e}\Delta T_e + \frac{\partial\varepsilon_1}{\partial T_p}\Delta T_p$$
$$+ i\left(\frac{\partial\varepsilon_2}{\partial T_e}\Delta T_e + \frac{\partial\varepsilon_2}{\partial T_p}\Delta T_p\right), \tag{1}$$

where the functional dependence of ε is dropped for clarity. The change in reflectance can be related to the dielectric functions by[14]

$$\frac{\Delta R}{R} = \frac{1}{R}\left[\frac{\partial R}{\partial\varepsilon_1}\Delta\varepsilon_1 + \frac{\partial R}{\partial\varepsilon_2}\Delta\varepsilon_2\right]. \tag{2}$$

By substituting Eq. (2) into Eq. (1), the reflectance can be simplified to the familiar thermoreflectance equation[3,13]

$$\frac{\Delta R}{R} = a\Delta T_e + b\Delta T_p, \tag{3}$$

where $a \propto \partial R/\partial T_e$ and $b \propto \partial R/\partial T_p$. This reflectance model directly relates the change in reflectance to the change in electron and phonon temperatures. The coefficients a and b are usually determined by fitting predicted changes in temperature from various models, such as the two temperature model (TTM),[15] to thermoreflectance data.[3,13]

The thermoreflectance model presented in Eq. (3) is dependent on the fact that ΔT_e and $\Delta T_p < 150$ K. This is easy to ensure at very low incident laser fluences, but with the wide spread use of more powerful lasers and higher laser fluences, the large changes in electron temperature will yield Eq. (3) inapplicable. Smith and Norris[16] developed a reflectance model that expands the range of temperature applicability of Eq. (3) in the event that only intraband transitions are excited, which simplifies the analysis since only the intraband contribution to the dielectric function must be considered. This intraband reflectance model is particularly useful in analyses involving noble metals since noble metals have a very distinct, high energy interband transition threshold (ITT) since the s-band/d-band crossing is significantly lower than the Fermi level. The lowest energy d-band to available s-band transition is very large for Cu (2.15 eV), Au (2.4 eV), and Ag (4 eV), making it easy to isolate the effects of the intraband transitions on thermoreflectance.[17] Transition metals, in contrast, pose a greater problem in isolating the various transitions and determining their dependencies on electron-phonon energy transfer through TTR since characteristically, transition metal band structures are shifted from the noble metals, so the s-band/d-band crossing is at or above the Fermi level. This produces several allowable low energy d-band (d_1-band) to s-band transitions, making it imperative to take into account interband transitions to analyze thermoreflectance. For example, Cr has Fermi transitions at 0.8 (ITT), 1.0, 1.4, and 1.6 eV, W has transitions at 0.85 (ITT), 1.6, and 1.75 eV,[18] and Ni has transitions at 0.25 (ITT), 0.4, and 1.3 eV.[19]

The key to thermoreflectance models lies in separating the complex dielectric function into the intra- and interband components. It has been shown that the complex dielectric function can be expressed as[20,21]

$$\varepsilon = \varepsilon^{(f)} + \varepsilon^{(b)}, \tag{4}$$

which explicitly separates the intraband effects [free electron effects denoted by the superscript (f)] from interband effects [bound-electron effects denoted by the superscript (b)]. Both $\varepsilon^{(f)}$ and $\varepsilon^{(b)}$ are complex expressions with real and imaginary parts. Therefore, Eq. (4) can be rewritten in the form of Eq. (1), where $\varepsilon_1 = \varepsilon_1^{(f)} + \varepsilon_1^{(b)}$ and $\varepsilon_2 = \varepsilon_2^{(f)} + \varepsilon_2^{(b)}$.

In the case that only intraband transitions are excited, a metal is irradiated with photons where the incident photon energy is less than the ITT, i.e., $\hbar\omega < $ ITT. In this case, the change in reflectance of the metal is dominated by the intraband transitions from the free electrons (since there is not enough energy in the incident photons to excite the bound electrons to undergo an interband transition). Therefore, $\varepsilon = \varepsilon^{(f)}$. The free electron dielectric function for this metal is described by the free electron or Drude model given by[22–24]

$$\varepsilon^{(f)} = 1 - \frac{\omega_{plasma}^2}{\omega(\omega + i\omega_\tau)} = 1 - \frac{\omega_{plasma}^2}{(\omega^2 + \omega_\tau^2)} + i\frac{\omega_\tau\omega_{plasma}^2}{\omega(\omega^2 + \omega_\tau^2)}, \tag{5}$$

where ω is the frequency of the incident photons, ω_{plasma} is the plasma frequency of the free electrons, and ω_τ is the collisional frequency of free electrons excited by the incident photons. In order to relate the dielectric function, and therefore the reflectance, to the electron and phonon temperatures, the temperature dependence of ω_τ must be exploited. This collisional frequency is inversely proportional to electron relaxation time, and therefore Matthiessen's rule[25] can be used to express the free electron collisional frequency as[26]

$$\omega_\tau \approx \frac{1}{\tau} = A_{ee}T_e^2 + B_{ep}T_p, \tag{6}$$

where A_{ee} and B_{ep} are the material constants relating to the temperature dependencies of the electron-electron and electron-phonon collisional frequencies.[26–28] Smith and Norris[16] exploited this relationship between the metal's reflectivity and the dielectric function to derive a thermoreflectance model that explicitly takes into account the change in electron and phonon temperatures during intraband transitions.

The reflectivity of a solid is calculated by the well known relationship[29]

$$R = \frac{(n_1 - 1)^2 + n_2^2}{(n_1 + 1)^2 + n_2^2}, \tag{7}$$

where n_1 and n_2 are the real and imaginary parts of the index of refraction n, which, in the case of intraband excitations only, is related to the complex dielectric function by

$$n = n_1 + in_2 = \sqrt{\varepsilon^{(f)}}. \tag{8}$$

However, to calculate the change in reflectivity ΔR as a function of change in temperature during nonequilibrium heating, the response of the indices of refraction due to temperature changes must be exploited. The temperature dependency of the dielectric function is used in Eq. (6), so the indices of refraction as a function of temperature are given by

$$n_1(T_e, T_p) = \text{Re}\sqrt{\varepsilon^{(f)}(T_e, T_p)}, \tag{9}$$

$$n_2(T_e,T_p) = \mathrm{Im}\sqrt{\varepsilon^{(f)}(T_e,T_p)}. \tag{10}$$

Equations (9) and (10) can then be used with Eq. (7) to determine the change in reflectivity ΔR with a change in electron and phonon temperature, which is calculated by

$$\Delta R(\Delta T_e,\Delta T_p) = R(T_e+\Delta T_e,T_p+\Delta T_p) - R(T_e,T_p) = \frac{[n_1(T_e+\Delta T_e,T_p+\Delta T_p)-1]^2 + n_2^2(T_e+\Delta T_e,T_p+\Delta T_p)}{[n_1(T_e+\Delta T_e,T_p+\Delta T_p)+1]^2 + n_2^2(T_e+\Delta T_e,T_p+\Delta T_p)}$$

$$- \frac{[n_1(T_e,T_p)-1]^2 + n_2^2(T_e,T_p)}{[n_1(T_e,T_p)+1]^2 + n_2^2(T_e,T_p)}. \tag{11}$$

$\Delta R/R$ is calculated by dividing Eq. (11) by Eq. (7) since Eq. (7) gives the baseline reflectivity at a given electron and phonon temperature and Eq. (11) determines how much this baseline reflectance changes as a result of changes in electron and phonon temperatures. Therefore, the change in reflectivity as a function of the change in temperature can be calculated by

$$\frac{\Delta R}{R} = \Delta R(\Delta T_e,\Delta T_p)\frac{[n_1(T_e,T_p)+1]^2 + n_2^2(T_e,T_p)}{[n_1(T_e,T_p)-1]^2 + n_2^2(T_e,T_p)}$$

$$= f[\varepsilon^{(f)}] = f(\omega_\tau) = f(A_{ee},B_{ep}), \tag{12}$$

where $\Delta R(\Delta T_e,\Delta T_p)$ is given by Eq. (11). The fitting procedure for this intraband reflectance model to thermoreflectance data is similar to that of the standard reflectance model in Eq. (3), only the constants A_{ee} and B_{ep} in the ω_τ term are determined from the fit.[16]

The intraband reflectance model is suited to study changes in reflectance due to changes in electron and phonon temperatures at any given temperature. However, in the event that the film thickness is approximately the same as the optical penetration depth $\delta = \lambda/(4\pi n_2)$, where λ is the wavelength of the incident photons, the reflectivity on the surface of the film is affected by the substrate, and therefore, the standard reflectivity equation given by Eq. (7) must be modified to take into account the optical properties of the substrate. Consequently, the intraband reflectance model must be modified. In this case, the reflectance must be calculated using the equations derived by Abeles.[30] Abeles developed reflectance expressions for various absorbing/nonabsorbing film/substrate combinations. In this thickness-dependent model, knowledge of the medium, film, and substrate indices of refraction along with film thickness and incident photon wavelength is needed to determine the reflectivity. To determine $\Delta R/R$, the model of Abeles[30] is evaluated using Eqs. (9) and (10) to calculate ΔR, then evaluated again with the values for the indices of refraction at the equilibrium temperature of interest to calculate R. Figure 1 shows calculations of $\Delta R/R$ for a 10, 30, and 50 nm Au film on a SiO$_2$ substrate in air at 300 K as a function of change in electron temperature and assuming the phonon temperature is kept constant at 300 K using the equations of Abeles[30] for an absorbing film on a nonabsorbing substrate [see Eqs. (A1)–(A10) in the Appendix]. In calculations in this work, the baseline reflectivity is always assumed at 300 K, and the change in electron temperature (from, for example, a short

pulsed laser) gives rise to ΔR. The assumption of a minimal change in phonon temperature is valid immediately after pulsed laser heating (before any significant electron-phonon energy transfer), which is the time regime of interest in this work. For Au, A_{ee} and B_{ep} are approximated as 1.2×10^7 and 1.23×10^{11} K^{-1} s^{-1},[27,31] respectively, and their temperature dependence is negligible in the electron temperature range of interest in this work (300–3500 K).[32] The plasma (angular) frequency of Au is 1.37×10^{16} rad s^{-1} (plasma energy of 9.03 eV).[33] Since the plasma frequency of a metal is given by $\omega_{\mathrm{plasma}}^2 = (4\pi n_e e^2/m)$ and n_e, e, and m—which are the conduction band electron number density, the fundamental charge, and the mass of an electron, respectively—are all constant assuming no interband (d-band to conduction band excitations) transitions, which would change the electron number density in the conduction band,[34,35] then the plasma frequency is assumed as temperature independent in the temperature range of interest. The nonlinearity of $\Delta R/R$ with change in electron temperature and the obvious thickness dependence is apparent in Fig. 1. The inset of Fig. 1 shows the change in the baseline reflectivity R as a function of film thickness. Bulk values for indices of refraction n_1 and n_2 are used for the substrates of interest in calculations in this work.[36]
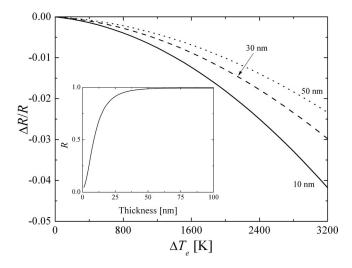

FIG. 1. Thickness dependence of $\Delta R/R$ in Au films on SiO$_2$ substrates as a function of electron temperature assuming a phonon system temperature at 300 K. The inset shows the baseline reflectivity R for an Au film on an SiO$_2$ substrate at 300 K using the reflectance model in the Appendix.
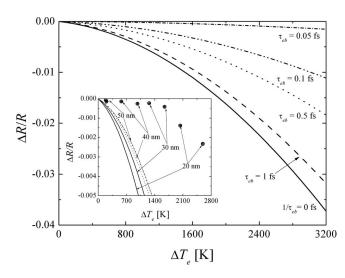
FIG. 2. $\Delta R/R$ as a function of temperature for a 30 nm Au films on a SiO$_2$ substrate for four different electron-boundary scattering times (τ_{eb} =1.0, 0.5, 0.1, and 0.05 fs) along with $\Delta R/R$ calculations assuming no substrate interference ($1/\tau_{eb}$=0). The inset compares $\Delta R/R$ measurements on a range of Au thin films on SiO$_2$ substrates by Hopkins et al. (Ref. 7) to $\Delta R/R$ calculated with the thickness-dependent intraband transition model using Eq. (6) for the electron collisional frequency.
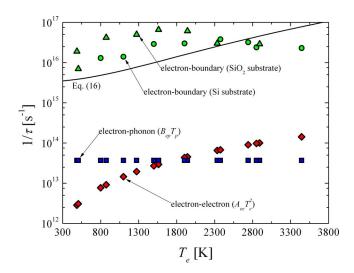

FIG. 3. (Color online) Electron-electron, electron-phonon, and electron-substrate scattering rates. The electron-electron and electron-phonon scattering rates are calculated by $1/\tau_{ee}=A_{ee}T_e^2$ and $1/\tau_{ep}=B_{ep}T_p$, respectively. The electron-substrate scattering rates are predicted by fitting the intraband thickness-dependent model for $\Delta R/R$ [using Eq. (13) for the electron collisional frequency and $1/\tau_{eb}$ as the adjustable parameter] to the maximum $\Delta R/R$ at the electron temperature reported by Hopkins et al. (Ref. 7) Results of $1/\tau_{eb}$ from this fit agree well with the electron-boundary scattering rate in the event of an electron-phonon nonequilibrium given by Eq. (16).

III. EFFECTS OF ELECTRON-BOUNDARY SCATTERING ON $\Delta R/R$

Although the thickness-dependent intraband reflectance model accounts for multiple reflection off the film/substrate interface by the absorbed radiation, it does not take into account electron scattering events at boundaries that will affect the electron collision frequency discussed in Eq. (6). Hopkins et al.[7] showed that during an electron-phonon nonequilibrium, electrons can inelastically scatter at a film-substrate boundary or at disordered regions in thin films near interfaces, thereby creating another path of energy loss for the electrons system in the thin film. These additional inelastic boundary scattering events would create another change in the electron collisional frequency, so Eq. (6) becomes

$$\omega_\tau = \frac{1}{\tau} \approx A_{ee}T_e^2 + B_{ep}T_p + \frac{1}{\tau_{eb}}, \qquad (13)$$

where τ_{eb} is some electron-boundary scattering time, such as that at the film-substrate interface. Using Eq. (13) instead of Eq. (6) in the intraband thickness-dependent reflectance model gives a relation between the thermoreflectance response in a metal undergoing intraband excitations and electron-boundary scattering causing a change in ΔR. Figure 2 shows $\Delta R/R$ as a function of temperature for a 30 nm Au films on a SiO$_2$ substrate for four different electron-boundary scattering times (τ_{eb}=1.0, 0.5, 0.1, and 0.05 fs) along with $\Delta R/R$ calculations assuming no substrate interference ($1/\tau_{eb}$=0). The trends in $\Delta R/R$ show that additional electron scattering processes decrease the magnitude of $\Delta R/R$. This is also apparent from comparing the maximum $\Delta R/R$ as a function of predicted electron temperature from the samples in Ref. 7 to $\Delta R/R$ calculated with the thickness-dependent intraband transition model using Eq. (6) for the electron collisional frequency (inset, Fig. 2). The low magnitude and different curvature of the measured $\Delta R/R$ could have re-

sulted from electron-boundary scattering events, where the models for $\Delta R/R$ in the inset only take into account electron-electron and electron-phonon scattering events.

To quantify the effects of electron-boundary scattering during laser pulse excitation, Eq. (13) is used in the thickness-dependent intraband transition model, and $1/\tau_{eb}$ is adjusted until the predicted $\Delta R/R$ matches the measured $\Delta R/R$ by Hopkins et al. for a given film-substrate sample at the predicted maximum electron temperature. Figure 3 shows the $1/\tau_{eb}$ predictions as a function of maximum electron temperature predicted by the TTM (Ref. 15) along with the other electron scattering terms in Eq. (13) assuming T_p =300 K. This shows the functional form of $1/\tau_{eb}$ with electron temperature, and based on the $\Delta R/R$ analysis, $1/\tau_{eb}$ should increase with electron temperature. The analysis in Ref. 7 using the three temperature model[37] predicted an increase in electron-interface energy transfer with electron temperature, which supports the trends seen in electron-boundary scattering in Fig. 3. In addition, $1/\tau_{eb}$ is approximately three orders of magnitude greater than the electron-electron and electron-phonon scattering rates.

Sergeev[38] derived an expression for electron–"vibrating" boundary scattering rate in disordered metallic conductors when the electrons and phonons are defined by the same temperature given by

$$\frac{1}{\tau_{eb}} = \frac{3\pi}{35\zeta(3)q_t\ell_{ep}\tau_{ep}}\left[1 + 2\left(\frac{v_L}{v_T}\right)^3\right], \qquad (14)$$

where $\zeta(s)$ is the Riemann–Zeta function, q_t is the dominant wavevector of the thermal longitudinal phonons, ℓ_{ep} is the mean free path of electron-phonon scattering events, $1/\tau_{ep}$ is the electron-phonon scattering rate in the corresponding bulk, "ordered" (no scattering at a vibrating boundary or interface) material, v_L is the group velocity of the longitudinal

phonons, and v_T is the group velocity of the transverse phonons. Note that only acoustic phonons are considered in Eq. (14) since optical phonons have near-zero group velocity. After a short pulsed laser heating event, both electron-electron and electron-phonon scattering events will affect electron relaxation, so in the event of an electron-phonon nonequilibrium after pulse absorption, the electron-boundary scattering rate is given by

$$\frac{1}{\tau_{eb}} = \frac{3\pi(A_{ee}T_e^2 + B_{ep}T_p)}{35\zeta(3)q_t\ell_{ee,ep}}\left[1 + 2\left(\frac{v_L}{v_T}\right)^3\right], \tag{15}$$

where $\ell_{ee,ep}$ is the electron mean free path, taking into account electron-electron and electron-phonon scattering. From kinetic theory, $\ell_{ee,ep} \approx v_L/(A_{ee}T_e^2 + B_{ep}T_p)$, so the rate of electron-boundary scattering after short pulsed laser heating is given by

$$\frac{1}{\tau_{eb}} = \frac{3\pi(A_{ee}T_e^2 + B_{ep}T_p)^2}{35\zeta(3)q_t v_L}\left[1 + 2\left(\frac{v_L}{v_T}\right)^3\right]. \tag{16}$$

Equation (16) is calculated as a function of electron temperature and is presented in Fig. 3 for the Au films of interest, assuming that $T_p = 300$ K and the phonon group velocities[39] are given by $v_L = 3390$ m s^{-1} and $v_T = 1290$ m s^{-1}. Since the lattice system is above the Debye temperature of Au ($\theta_D = 165$ K),[40] $q_t = k_B\theta_D/(hv_L)$, where k_B is Boltzmann's constant and h is Planck's constant. Equation (16) shows good agreement in magnitude and trends of $1/\tau_{eb}$ predicted from the $\Delta R/R$ data.

The deviations of Eq. (16) from the data could be due to other electron scattering mechanisms not taken into account in this study. The formulation of Eq. (13) assumes that electron-electron, electron-phonon, and electron-boundary scatterings are the sole electron scattering mechanisms that affect thermoreflectance. However, using Matthiessen's rule, the effects of other electron dephasing mechanisms on thermoreflectance can be considered. For example, electron-impurity scattering is described by replacing the electron mean free path in Eq. (14) with the characteristic dimension of the material.[38,41] Therefore, electron-impurity scattering after short pulsed laser heating is given by

$$\frac{1}{\tau_{ei}} = \frac{3\pi(A_{ee}T_e^2 + B_{ep}T_p)}{35\zeta(3)q_t d}\left[1 + 2\left(\frac{v_L}{v_T}\right)^3\right], \tag{17}$$

where d is the film thinkess. In the temperature range of interest, the electron-impurity scattering rate predicted by

Eq. (17) is of the order of 10^{13}–10^{14}, of the same order as the electron-electron and electron-phonon scattering rates, but still three orders of magnitude less than the electron-boundary scattering rate. Therefore, in thin films where film/substrate interface scattering is significant, this scattering mechanism will be the dominant contribution to the change in the thermoreflectance signal. However, as film/substrate interface scattering becomes less pronounced, other electron dephasing mechanisms can affect thermoreflectance, such as electron-impurity scattering.

In conclusion, electron-boundary scattering after ultrashort pulse absorption in thin metal films can drastically affect the change in reflectance induced from the laser heating. To take electron-boundary scattering into account, an additional scattering term is introduced into the Drude model for the complex dielectric function. Using an intraband thickness-dependent reflectance model, transient thermoreflectance data of Au films subject to intraband excitations are analyzed with the electron-boundary scattering Drude model introduced in this work. The electron-boundary scattering rate is determined from the Au data, showing that after short pulsed laser heating, electron-boundary scattering rates can be almost three orders of magnitude greater than the electron-electron and electron-phonon scattering rates. The scattering rates determined from the thermoreflectance data agree well with the theoretical predictions for electron-boundary scattering calculated from an electron-boundary scattering model for disordered conductors in the event of an electron-phonon nonequilibrium.

ACKNOWLEDGMENTS

APPENDIX: SURFACE REFLECTIVITY OF A THIN FILM ON A SUBSTRATE

The reflectivity of the Au/substrate samples examined in this work can be calculated with the equation for reflectivity of an absorbing film on a nonabsorbing substrate derived by Abeles[30] and given by

$$R = \frac{a'b'\exp[2n_2f'] + c'd'\exp[-2n_2f'] + 2q'\cos[2n_1f'] + 2s'\sin[2n_1f']}{b'd'\exp[2n_2f'] + a'c'\exp[-2n_2f'] + 2t'\cos[2n_1f'] + 2u'\sin[2n_1f']}, \tag{A1}$$

where

$$a' = (n_1 - n_{1,0})^2 + n_2^2, \tag{A2}$$

$$b' = (n_1 + n_{1,s})^2 + n_2^2, \tag{A3}$$

$$c' = (n_1 - n_{1,s})^2 + n_2^2, \tag{A4}$$

$$d' = (n_1 + n_{1,0})^2 + n_2^2, \tag{A5}$$

$$f' = 2\pi d/\lambda, \tag{A6}$$

$$q' = (n_{1,0}^2 + n_{1,s}^2)(n_1^2 + n_2^2) - (n_1^2 + n_2^2)^2 - n_{1,0}^2 n_{1,s}^2$$
$$- 4n_{1,0}n_{1,s}n_2^2, \tag{A7}$$

$$s' = 2n_2(n_{1,s} - n_{1,0})(n_1^2 + n_2^2 + n_{1,0}n_{1,s}), \tag{A8}$$

$$t' = (n_{1,0}^2 + n_{1,s}^2)(n_1^2 + n_2^2) - (n_1^2 + n_2^2)^2 - n_{1,0}^2 n_{1,s}^2$$
$$+ 4n_{1,0}n_{1,s}n_2^2, \tag{A9}$$

$$u' = 2n_2(n_{1,s} + n_{1,0})(n_1^2 + n_2^2 - n_{1,0}n_{1,s}), \tag{A10}$$

and $n_{1,s}$ and $n_{1,0}$ refer to the real part of the index of refraction of the substrate and ambient, respectively.

[1] D. G. Cahill, W. K. Ford, K. E. Goodson, G. D. Mahan, A. Majumdar, H. J. Maris, R. Merlin, and S. R. Phillpot, J. Appl. Phys. **93**, 793 (2003).

[2] S. D. Brorson, J. G. Fujimoto, and E. P. Ippen, Phys. Rev. Lett. **59**, 1962 (1987).

[3] S. D. Brorson, A. Kazeroonian, J. S. Moodera, D. W. Face, T. K. Cheng, E. P. Ippen, M. S. Dresselhaus, and G. Dresselhaus, Phys. Rev. Lett. **64**, 2172 (1990).

[4] N. Del Fatti, C. Voisin, M. Achermann, S. Tzortzakis, D. Christofilos, and F. Vallée, Phys. Rev. B **61**, 16956 (2000).

[5] G. V. Hartland, Int. J. Nanotechnol. **1**, 307 (2004).

[6] J. Hohlfeld, S. S. Wellershoff, J. Gudde, U. Conrad, V. Jahnke, and E. Matthias, Chem. Phys. **251**, 237 (2000).

[7] P. E. Hopkins, J. L. Kassebaum, and P. M. Norris, J. Appl. Phys. **105**, 023710 (2009).

[8] P. E. Hopkins, J. M. Klopf, and P. M. Norris, Appl. Opt. **46**, 2076 (2007).

[9] C. K. Sun, F. Vallee, L. Acioli, E. P. Ippen, and J. G. Fujimoto, Phys. Rev. B **48**, 12365 (1993).

[10] C. K. Sun, F. Vallee, L. Acioli, E. P. Ippen, and J. G. Fujimoto, Phys. Rev. B **50**, 15337 (1994).

[11] R. Rosei and D. W. Lynch, Phys. Rev. B **5**, 3883 (1972).

[12] H. Hirori, T. Tachizaki, O. Matsuda, and O. B. Wright, Phys. Rev. B **68**, 113102 (2003).

[13] P. M. Norris, A. P. Caffrey, R. J. Stevens, J. M. Klopf, J. T. McLeskey, and A. N. Smith, Rev. Sci. Instrum. **74**, 400 (2003).

[14] W. J. Scouler, Phys. Rev. Lett. **18**, 445 (1967).

[15] S. I. Anisimov, B. L. Kapeliovich, and T. L. Perel'man, Sov. Phys. JETP **39**, 375 (1974).

[16] A. N. Smith and P. M. Norris, Appl. Phys. Lett. **78**, 1240 (2001).

[17] G. L. Eesley, Phys. Rev. B **33**, 2144 (1986).

[18] E. Colavita, A. Franciosi, C. Mariani, and R. Rosei, Phys. Rev. B **27**, 4684 (1983).

[19] J. Hanus, J. Feinleib, and W. J. Scouler, Phys. Rev. Lett. **19**, 16 (1967).

[20] H. Ehrenreich and H. R. Philipp, Phys. Rev. **128**, 1622 (1962).

[21] H. Ehrenreich, H. R. Philipp, and B. Segall, Phys. Rev. **132**, 1918 (1963).

[22] R. Hummel, *Electronic Properties of Materials*, 2nd ed. (Springer, New York, 1997).

[23] M. I. Markovic and A. D. Rakic, Appl. Opt. **29**, 3479 (1990).

[24] M. I. Markovic and A. D. Rakic, Opt. Laser Technol. **22**, 394 (1990).

[25] J. M. Ziman, *Electrons and Phonons* (Clarendon, Oxford, 1960).

[26] N. W. Ashcroft and N. D. Mermin, *Solid State Physics* (Saunders College, Fort Worth, 1976).

[27] A. H. MacDonald, Phys. Rev. Lett. **44**, 489 (1980).

[28] D. S. Ivanov and L. V. Zhigilei, Phys. Rev. B **68**, 064114 (2003).

[29] G. Laufer, *Introduction to Optics and Lasers in Engineering* (Cambridge University Press, Cambridge, 1996).

[30] F. Abeles, in *Advanced Optical Techniques*, edited by A. C. S. V. Heel (North-Holland, Amsterdam, 1967), pp. 145–188.

[31] X. Y. Wang, D. M. Riffe, Y.-S. Lee, and M. C. Downer, Phys. Rev. B **50**, 8016 (1994).

[32] M. Kaveh and N. Wiser, Adv. Phys. **33**, 257 (1984).

[33] A. D. Rakic, A. B. Djurisic, J. M. Elazar, and M. L. Majewski, Appl. Opt. **37**, 5271 (1998).

[34] P. E. Hopkins, J. C. Duda, R. N. Salaway, J. L. Smoyer, and P. M. Norris, Nanoscale Microscale Thermophys. Eng. **12**, 320 (2008).

[35] Z. Lin, L. V. Zhigilei, and V. Celli, Phys. Rev. B **77**, 075133 (2008).

[36] E. D. Palik, *Handbook of Optical Constants of Solids* (Academic, Orlando, 1985).

[37] P. E. Hopkins and P. M. Norris, Appl. Surf. Sci. **253**, 6289 (2007).

[38] A. V. Sergeev, Phys. Rev. B **58**, R10199 (1998).

[39] D. E. Gray, *American Institute of Physics Handbook*, 3rd ed. (McGraw-Hill, New York, 1972).

[40] C. Kittel, *Introduction to Solid State Physics*, 7th ed. (Wiley, New York, 1996).

[41] N. G. Ptitsina, G. M. Chulkova, K. S. Il'in, A. V. Sergeev, F. S. Pochinkov, E. M. Gershenzon, and M. E. Gershenson, Phys. Rev. B **56**, 10089 (1997).